arXiv:hep-lat/9709114v1 25 Sep 1997

# The Structure of Flux Tubes in Maximal Abelian Gauge

Christoph Schlichter[a*], Gunnar S. Bali[b], and Klaus Schilling[c]

[a]Fachbereich Physik, Bergische Universität, D-42097 Wuppertal, Germany

[b]Physics Department, The University, Highfield, Southampton SO17 1BJ, United Kingdom

[c]HLRZ c/o Forschungszentrum Jülich, D-52425 Jülich and DESY, 22603, Hamburg, Germany

Various field strength correlators are investigated in the maximal abelian projection of pure SU(2) lattice gauge theory. High precision measurements of the colour fields, monopole currents, their curl and divergence allow for detailed checks of the dual superconductor scenario. A further decomposition of abelian observables into monopole and photon parts reveals that the flux tube is built up from the monopole part alone.

## 1. INTRODUCTION

Almost 20 years ago, 't Hooft and Mandelstam proposed the dual superconductor scenario of confinement: it is believed that at low temperature magnetic monopoles condense and thus, chromo electric flux is expelled from the QCD vacuum, analogous to a type II superconductor. This leads to the formation of thin electric flux tubes between colour charges and thus to a linearly rising potential, explaining confinement. In view of both, making genuinely non perturbative aspects of QCD accessible to analytical treatment and understanding how confinement arises, it is worthwhile to investigate to what extent QCD reproduces expectations from the Ginzburg-Landau (GL) equations, and to fix their relevant parameters. Pioneering steps in this direction have been made in Refs. [1,2].

In nonabelian theories, the definition of fields and currents becomes ambiguous. 't Hooft suggested the maximal abelian gauge as a renormalizable gauge condition for projecting out a Cartan subgroup, believed to be relevant for infra red aspects of QCD (abelian dominance). In this investigation, we follow these lines. Previously, the abelian string tension has been found to reproduce the nonabelian one within 8% [3,4]. A further decomposition of the abelian Wilson loop into photon and monopole parts [5] shows that the monopole part accounts exclusively for the string tension [6,4]. Here we extend these studies to the level of field distributions.

## 2. SIMULATION

We investigate a $32^4$ lattice at $\beta = 2.5115$, corresponding to a lattice spacing $a \approx 0.086$ fm, where the scale has been set from the string tension value $\sqrt{\kappa} = 440$ MeV. A careful study of systematic errors introduced by incomplete gauge fixing and optimisation of the gauge fixing procedure are crucial for obtaining reliable results. We take measurements on 108 independent abelian configurations, generated in the context of Ref. [4]. In the limit of large $T$, we measure connected correlation functions [7],

$$\langle O(\mathbf{x},T)\rangle = \frac{\langle O(\mathbf{x},T/2)W(R,T)\rangle}{\langle W(R,T)\rangle} - \langle O\rangle. \qquad (1)$$

By varying $\mathbf{x}$, we scan through the space around two static sources, separated by a distance $Ra$. Depending on the type of the local probe $O$, distributions of $\mathbf{E}$, $\mathbf{B}$, $\nabla^+ \wedge \mathbf{E}$, $\nabla^- \wedge \nabla^+ \wedge \mathbf{E}$, $\mathbf{J}_m$ and $\nabla^- \wedge \mathbf{J}_m$ are obtained. $W$ denotes a smeared Wilson loop, which is either built up from abelian link angles or from the regular (photon) or the singular (monopole) contributions to these angles alone, according to the approximate factorisation of Ref. [4].

---

[*] Talk presented by Christoph Schlichter.

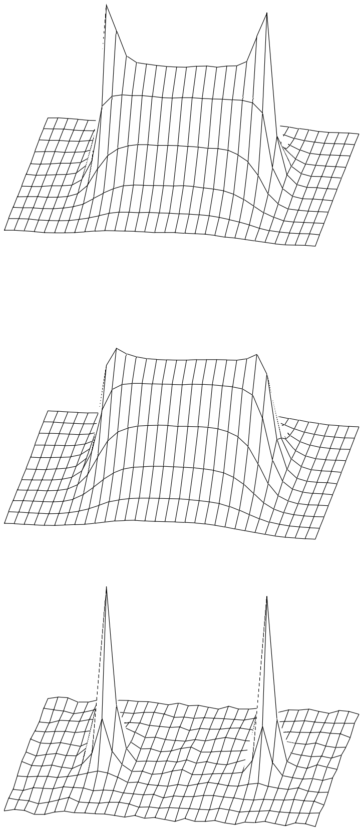

Figure 1. Abelian action density: full distribution, monopole and photon contributions, respectively.

## 3. MONOPOLE CONTRIBUTION

It has been demonstrated previously that the abelian potential approximately factorises into a monopole and a photon contribution [6,4]. Here, we investigate this factorisation on the level of the underlying field distributions. In Fig. 1 the situation is depicted for the action density, $\sigma = 1/2(\mathbf{E}^2 - \mathbf{B}^2)$. In accord with naïve expectations, the string is entirely due to the monopole part, whereas the effect of the photon part is localised in the vicinity of the sources[2].

## 4. DUAL SUPERCONDUCTIVITY

We choose the coordinates such that the colour sources lie on the $z$-axis at positions $z = \pm r/2$ with $r = Ra$. $x_\perp = (x^2 + y^2)^{1/2}$ denotes the transverse distance from the interquark string. A combination of Ampere's law $\nabla \wedge \mathbf{E} = \mathbf{J}_m$ with the London equation $\mathbf{A} + \lambda^2 \mathbf{J}_m = 0$ yields $E_z(x_\perp) - \lambda^2 \Delta_\perp E_z(x_\perp) = \Phi_m \delta^2(x_\perp)$. We expect the analytical solution,

$$E_z = \frac{\Phi_m}{2\pi\lambda^2} K_0(x_\perp/\lambda), \qquad (2)$$

to hold in the London limit which should be realized at sufficiently large $r$ and $x_\perp$. For $T \geq 6$, we find all our data on $\nabla^+ \wedge \mathbf{E}$ and $\mathbf{J}_m$ to be in perfect agreement with Ampere's law and proceed to fit $E_z$ in the central plane ($z = 0$) to Eq. (2) as a test of the validity of the London equation.

Table 1
Fits of $E_z$ at $R = 8$ according to Eq. (2).

| range | $\Phi_m$ | $\lambda$ | $\chi^2$/dof |
|---|---:|---:|---:|
| 1…7.07 | 2.2(3) | 3.6(5) | 1700 |
| 2…7.07 | 1.7(1) | 2.4(1) | 150 |
| 3…7.07 | 1.7(1) | 2.0(1) | 6 |
| 3.1…7.07 | 1.8(1) | 2.0(1) | 9 |
| 3.6…7.07 | 1.9(1) | 1.9(1) | 4 |
| 4…7.07 | 2.0(1) | 1.88(6) | 1.8 |
| 4.2…7.07 | 1.9(1) | 1.82(7) | 1.2 |
| 4.5…7.07 | 2.0(1) | 1.82(2) | 1.1 |
| 5…7.07 | 2.1(1) | 1.66(7) | 0.7 |

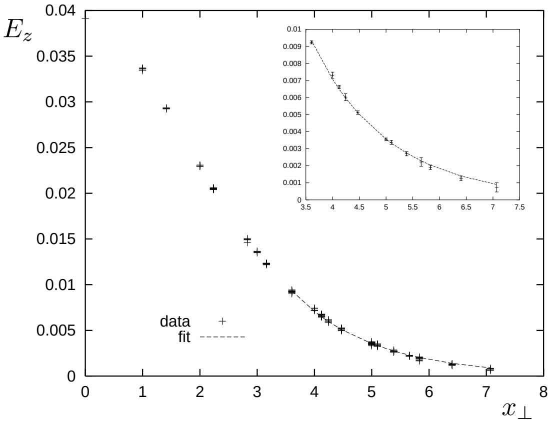

Figure 2. Fit of $E_z$ to Eq. (2) (for $R = 10$).

---

[2] A database of colour images can be accessed via anonymous ftp from wpts0.physik.uni-wuppertal.de. The compressed .rgb and .ps files are deposited in the directory /pub/MAcolorflux.

Results for various fit ranges are summarised in Table 1 for the example $R = 8$. For $x_\perp \geq 0.3$ fm, the fit parameters become stable and the $\chi^2$-values reasonable. One such fit (for $R = 10$) is displayed in Fig. 2. For all distances, we obtain penetration lengths of $\lambda \approx 0.15$ fm. The value of the external magnetic flux $\Phi_m$ is determined by the magnetic charge of the objects, into which the monopoles condense. Assuming the London limit to apply we find $\Phi_m \approx 2$.

We proceed to compare the small $x_\perp$ data directly to the expectation from dual GL equations that relate the vector potential $\mathbf{A}$, to the magnetic monopole current $\mathbf{J}_m$. The GL wave function $\psi = \psi_\infty f(x_\perp) e^{i\theta}$ and its coherence length $\xi$ enter the scenario. $f$ approaches zero as $x_\perp \to 0$. The London limit corresponds to $f(x_\perp) = 1$. This is the asymptotic value as $x_\perp \to \infty$. The ansatz $f(x_\perp) = \tanh(\nu r/\xi)$ approximately solves the nonlinear GL equations for these boundary conditions. A small-$x_\perp$ expansion yields $\nu = \sqrt{3/8}$. We determine the vector potential by numerically integrating the electric field,

$$A_\theta(x_\perp) = \frac{1}{x_\perp} \int_0^{x_\perp} dx'_\perp \, x'_\perp E_z(x'_\perp). \tag{3}$$

Subsequently, this data is fitted to,

$$A_\theta(x_\perp) = \frac{\lambda^2}{f(x_\perp)^2} J_{m,\theta}(x_\perp) - \frac{\Phi_m}{2\pi x_\perp}, \tag{4}$$

with parameters $\Phi_m$, $\xi$ and $\lambda$. $J_{m,\theta}$ is a parametrisation fitted to the angular component of the measured magnetic monopole current.

Table 2
Fits of $A_\theta$ and $J_{m,\theta}$ to Eq. (4) (at $R = 8$).

| $T$ | $\lambda$ | $\xi$ | $\Phi_m$ |
|---|---|---|---|
| 2 | 1.88(4) | 1.19(2) | 1.03(1) |
| 3 | 1.88(3) | 1.56(2) | 1.20(1) |
| 4 | 1.84(2) | 1.76(2) | 1.28(1) |
| 5 | 1.75(2) | 2.06(2) | 1.35(1) |
| 6 | 1.82(2) | 2.05(2) | 1.41(1) |

All data are well described by the fits. Results for the example $R = 8$, corresponding to a source separation $r \approx 0.7$ fm, are summarised in Table 2. The quality of the fit for $T = 6$ is visualised in Fig. 3. The difference between the $f = 1$ curve and the data indicates to what extent we are probing surface effects. The results on the penetration length nicely agree with results from Eq. (2). A plateau in $\xi$ is reached for $T \geq 5$. However, the value for $\Phi_m$ is not saturated yet; we obtain a lower limit, $\Phi_m \leq 1.4$. The ratio, $\lambda/\xi = 0.89(2)$ turns out to be definitely larger than the critical value $1/\sqrt{2}$, i.e. the SU(2) appears to act like a type II superconductor [8].

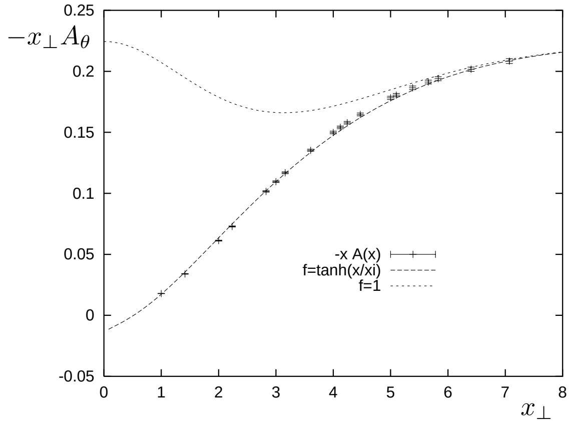

Figure 3. Check of Eq. (4) for $R = 8$, $T = 6$. The $f(x) = 1$ curve corresponds to the London limit.

## ACKNOWLEDGEMENTS

We acknowledge support by the DFG (grants Schi 257/1-4 and Schi 257/3-2), the EU (contracts SC1*-CT91-0642, CHRX-CT92-0051 and CHBG-CT94-0665) and PPARC (grant GR/K55738).

## REFERENCES

1. R. W. Haymaker et al., Phys. Lett. B306 (1993) 115.
2. P. Cea et al., Phys. Rev. D52 (1995) 5152.
3. H. Shiba et al., Phys. Lett. B333 (1994) 461.
4. G.S. Bali et al., Phys. Rev. D54 (1996) 2863.
5. J. Smit et al., Nucl. Phys. B355 (1991) 603.
6. H.D. Trottier et al., Phys. Rev. D53 (1995) 1532.
7. C. Schlichter et al., Phys. Rev. D51 (1995) 5165.
8. C. Schlichter, PhD-thesis Wuppertal (1997), G. Bali et al., to be published.